Development 137, 1585 (2009) doi:10.1242/dev.052373

The maize SBP-box transcription factor encoded by *tasselsheath4* regulates bract development and the establishment of meristem boundaries

George Chuck, Clinton Whipple, David Jackson and Sarah Hake

An error was published in *Development* **137**, 1243-1250.

In the second paragraph of the Discussion (on p. 1248), a figure was incorrectly cited.

The text should have read as follows:

“The derepressed bract growth also alters the apparent phyllotaxy, changing it from ordered rows to spiral by pushing the rows of spikelet pairs apart (Fig. 2F).”

The authors apologise to readers for this mistake.

Development 137, 1243-1250 (2010) doi:10.1242/dev.048348

The maize SBP-box transcription factor encoded by *tasselsheath4* regulates bract development and the establishment of meristem boundaries

George Chuck[1,*], Clinton Whipple[2], David Jackson[2] and Sarah Hake[1]

SUMMARY

Plant architecture consists of repeating units called phytomers, each containing an internode, leaf and axillary meristem. The formation of boundaries within the phytomer is necessary to differentiate and separate these three components, otherwise some will grow at the expense of others. The microRNA-targeted SBP-box transcription factor *tasselsheath4* (*tsh4*) plays an essential role in establishing these boundaries within the inflorescence. *tsh4* mutants display altered phyllotaxy, fewer lateral meristems and ectopic leaves that grow at the expense of the meristem. Double-mutant analyses of *tsh4* and several highly branched mutants, such as *ramosa1-3* and *branched silkless1*, demonstrated a requirement for *tsh4* in branch meristem initiation and maintenance. TSH4 protein, however, was localized throughout the inflorescence stem and at the base of lateral meristems, but not within the meristem itself. Double labeling of TSH4 with the *ramosa2*, *branched silkless1* and *knotted1* meristem markers confirmed that TSH4 forms a boundary adjacent to all lateral meristems. Indeed, double labeling of miR156 showed a meristem-specific pattern complementary to that of TSH4, consistent with *tsh4* being negatively regulated by this microRNA. Thus, downregulation of TSH4 by a combination of microRNAs and branching pathway genes allows the establishment of lateral meristems and the repression of leaf initiation, thereby playing a major role in defining meristem versus leaf boundaries.

KEY WORDS: Maize, Meristem, MicroRNA

INTRODUCTION

The shoot apical meristem forms at the apex of the plant and produces leaves at its flank. Lateral meristems form in the axils of leaves, and their number, rate of growth and determinacy pattern the general architecture of the plant. The leaf, lateral meristem and internode can collectively be considered as a unit, called a phytomer (Galinat, 1959). During the vegetative phase, the subtending leaf is large, whereas the axillary lateral meristem is small. Within the reproductive phase, however, the leaf portion of the phytomer, typically called the bract, is often repressed. Several studies indicate that control of cell fate within the phytomer plays a major role in the establishment of lateral organ architecture. For example, during the early stages of floral initiation in *Arabidopsis* there is a transient period during which cell fates are not fixed in lateral primordia. Such primordia can either form leaves or meristems depending on signals received from the environment and shoot apex (Hempel and Feldman, 1994; Hempel and Feldman, 1995). To date, the molecular nature of these signals and how they are perceived by the meristem to fix labile cell fates are unclear.

Bract suppression within the floral phase is a common feature found in dicotyledonous plants. For example, *Arabidopsis* bracts normally subtend floral meristems, but are later incorporated into the flower, leaving no morphological remnant (Heisler et al., 2005). Several *Arabidopsis* mutants, however, derepress bract development, including *leafy* (Weigel et al., 1992), *jagged* (Dinneny et al., 2004; Ohno et al., 2004), *ufo* (Hepworth et al., 2006) and *bop* (Hepworth et al., 2005; Norberg et al., 2005). Interestingly, all of these genes also function to control floral patterning, indicating that bract suppression and meristem function might be co-regulated.

Previous work on the dominant *Corngrass1* (*Cg1*) mutant of maize showed that SBP-box transcription factors control lateral organ development and cell fate within the inflorescence. *Cg1* is caused by the overexpression of miR156b/c, which results in inappropriate downregulation of several SBP-box genes during the floral phase (Chuck et al., 2007). *Cg1* displays juvenile leaves throughout development, as well as an unbranched tassel with ectopic vegetative leaves during the floral phase (Poethig, 1988). These data suggest that the loss of one or more SBP-box genes is responsible for the *Cg1* floral phenotype. Here, we provide evidence that *tasselsheath4* (*tsh4*) is caused by mutation of *zmSBP6*, a target of *Cg1* (Chuck et al., 2007). *tsh4* primarily functions to repress lateral organ growth, but also affects phyllotaxy, axillary meristem initiation and meristem determinacy within the floral phase. Double-mutant analysis shows that *tsh4* acts downstream of several genes responsible for the establishment of meristem determinacy, including *ramosa1* (*ra1*) (Vollbrecht et al., 2005), *ra2* (Bortiri et al., 2006), *ra3* (Satoh et al., 2006) and *branched silkess1* (*bd1*) (Chuck et al., 2002). Furthermore, because *tsh4* is a target of miR156, the location of miR156 expression relative to that of *tsh4* was analyzed, and found to be complementary. These results indicate that the establishment of lateral meristems leads to the expression of miR156, which in turn downregulates *tsh4* within the meristem, thus restricting TSH4 activity to the subtending bract, where it suppresses growth.

[1]Plant Gene Expression Center, United States Department of Agriculture-Agriculture Research Service and the University of California, Albany, CA 94710, USA. [2]Cold Spring Harbor Laboratory, 1 Bungtown Road, Cold Spring Harbor, NY 11724, USA.

*Author for correspondence (georgechuck@berkeley.edu)

Accepted 12 February 2010

MATERIALS AND METHODS

Isolation of *tsh4* alleles

The *tsh4-ref* allele was isolated from EMS-mutagenized W22 lines from the Maize Tilling Project (http://genome.purdue.edu/maizetilling/). The *tsh4-m1* allele was isolated from *Ds*-mutagenized W22 lines (http://www.plantgdb.org/prj/AcDsTagging/). The *tsh4-mum1* allele was isolated from Trait Utility System for Corn (TUSC) libraries (Bensen et al., 1995). Crosses between *tsh4-mum1* and either *tsh4-ref* or *tsh4-m1* resulted in a *tsh4* phenotype, demonstrating that they are allelic.

Phenotypic analysis

Double mutants were made between the *tsh4-mum1* allele and *ra1-ref*, *ra2-DM* and *ra3-ref*, and *bd1-glu* mutants by self-crossing the F1. *tsh4-mum1* homozygotes were selected by PCR using oligos 6F (5′-GAGCCGTTGACCTACTACTATTGGTCGTCT-3′) and 6R (5′-AAGCAGCATGGGAAGTCCGCAATGTTC-3′). *ra2-DM* mutants were selected using oligos full *ra2* F (5′-AAAAGAATTCCGTCCCCGTCGAGCACCA-3′) and full *ra2* R (5′-TTTTCTCGAGGCTGCTGTCTCCCCCTTC-3′). *ra1-r* mutants were selected using a linked *glossy* mutant marker, and by sequencing the *ra1* gene to identify homozygotes using primers *ra1* full F (5′-GCTCCCTCCATTTGTCCATTC-3′) and *ra1* R (5′-AGTTCGTTCCTCTGTCTGGCTC-3′). Double mutants for *ra3-ref* were made by self-crossing *ra3-ref* homozygous plants that were heterozygous for *tsh4-mum1* and screening for *tsh4-mum1* homozygotes by PCR. *bd1-glu* mutants were screened using oligos *bd1-7* (5′-ATGATGAATACCCGAGCCTGTGG-3′) and *bd1-9* (5′-GCGTGCGTGTAGACGAAGTTGG-3′).

All double mutants were repeated using different allelic combinations. The *tsh4-m1* allele was used to make doubles with *ra1-ref*, *ra2-DM* and *ra3-ref*, and *bd1-ref*. Similar phenotypic results were derived with both *tsh4* alleles.

Samples were fixed in formalin/acetic acid/alcohol (FAA) overnight, critical-point dried, sputter coated and examined as previously described (Chuck et al., 1998).

Molecular analysis of *tsh4*

The full-length *tsh4* cDNA was originally cloned from maize ear cDNA using primers corresponding to SBP-box clone *TC305894* (Chuck et al., 2007). Full-length genomic sequence was derived from the Maize Sequencing Project (maizesequence.org). Northern blot analysis was performed as previously described (Kerstetter et al., 1994), probing with the 3′ end of the *tsh4* cDNA outside the SBP domain. MicroRNA northern blots were performed as described (Chuck et al., 2007).

Cleavage assay

Polyadenylated RNA was isolated from 0.5 cm tassel primordia and 200 ng used directly for ligation to the GeneRacer 5′ RACE oligo and reverse transcribed (Invitrogen). One microliter of the reverse transcription reaction was used for RT-PCR using the GeneRacer 5′ oligo in combination with the SBP6 R1 oligo (5′-GCTGGTGGTGGAATGGTT-3′), which is located 320 bases from the microRNA binding site. The cleaved PCR product was cloned into pGEM-T Easy (Promega) and sequenced using M13 primers.

Generation of a TSH4 antibody, immunolocalization and double labeling

Sequence encoding the full-length TSH4 protein coupled to a HIS tag was cloned into the pET21d expression vector (Novagen). Recombinant protein was isolated under denaturing conditions, dialyzed and injected into rabbits (ProSci). The serum was affinity purified using either full-length TSH4 protein coupled to a GST tag (Novagen), or the C-terminus of TSH4 outside the SBP-box domain coupled to the GST tag. Similar results on western blots and immunolocalizations were obtained using both antibodies. Using the antibody to the full-length protein, a single band was detected in wild-type nuclear extracts but not in those from the *tsh4* mutant, indicating that the antibody is specific (see Fig. S1B in the supplementary material).

Immunolocalization was performed using previously described protocols (Jackson, 1991). To perform double labeling using RNA in situ probes, the in situ hybridization was performed first using previously described probes for *kn1* (Jackson, 1991), *ra2* (Bortiri et al., 2006), *bd1* (Chuck et al., 2002) and miR156 (Chuck et al., 2007) (Exiqon). After the alkaline phosphatase development step, the reaction was stopped by immersion in 1×PBS and further blocked in 0.1% BSA in PBS. A 1/100 dilution of TSH4 antibody was added to the slides and incubated overnight at 4°C. After three washes in blocking solution to remove primary antibody, an anti-rabbit biotinylated secondary antibody was added (Vector Labs) and incubated at room temperature for 1 hour. After washing as above, an anti-biotin tertiary antibody was added (Vector Labs) and incubated for 1 hour at room temperature. After washing as above, the slides were developed using the DAB staining system (Vector Labs), mounted in aqueous mounting media and photographed.

RESULTS

Normal maize development

Maize produces two types of inflorescence: the tassel and the ear (Fig. 1A,E). Upon the floral transition, the shoot apical meristem converts into a tassel primordium, which is located in a terminal position and contains male flowers, whereas ears are located in the axils of vegetative leaves and contain female flowers. The inflorescence meristem (IM) initiates a series of lateral meristems in a sequential ordered pattern. Only the tassel IM initiates branch meristems (BMs), whereas both the tassel and ear initiate spikelet pair meristems (SPMs) in a spiral phyllotaxy (Fig. 2A,C,E). Each SPM initiates a pair of spikelet meristems (SMs) in a distichous phyllotaxy (Fig. 2C,E). The SM initiates two sterile leaves, called glumes, followed by two lemmas, each of which contains a floral meristem in its axil (Cheng et al., 1983).

The *tsh4* mutant phenotype

A screen for mutants that cause derepression of bract growth within the maize inflorescence uncovered several alleles of *tsh4*. The mutants were all analyzed in a W22 background. *tsh4* mutant tassels typically had one to five long tassel branches, instead of ~13 as in wild type (Fig. 1A; Table 1). In place of tassel branches, long bract leaves were present, clustered at the base of the tassel (Fig. 1B; Table 1). Removal of these leaves revealed compression of the internodes, as if bract growth occurred at the expense of internode growth (Fig. 1C). Bract growth often occurred at the expense of lateral meristems of the tassel branch as well, as axillary tassel branches were often absent or highly reduced, consisting of only a few spikelets (Fig. 1D). In addition, solitary spikelets often appeared instead of spikelet pairs along the main rachis. Both solitary and paired spikelets were frequently subtended by bracts (Fig. 1F; Table 1). Since the maize ear does not have branches, these branching defects were not detectable in the ear. Derepressed bracts, however, were still visible at the base of the ear (Fig. 1E). In addition, the phyllotaxy of the kernel rows was different in *tsh4*, showing a near spiral phyllotaxy, instead of straight ordered rows of kernels as in wild type (Fig. 1E). These defects resulted from growth of the derepressed bracts subtending the spikelet pairs in the ear. The decrease in the number of BMs and spikelet pairs, and increase in the growth of lateral organs, suggested that TSH4 might regulate the decision as to whether lateral primordia are partitioned into either determinate or meristematic cells.

Several maize mutants display phenotypes opposite to those of *tsh4*, exhibiting an enhanced number of tassel branches. These include *ra1*, *ra2* and *ra3* (McSteen, 2006). All *ramosa* mutants display SPM indeterminacy, replacing spikelet pairs with branches or spikelet multimers containing extra spikelets. Thus, the *ramosa* genes function to impose determinate identities on the SPM (McSteen, 2006). *ra2* encodes a LOB-domain transcription factor (Bortiri et al., 2006) that controls the expression of RA1, a C2H2

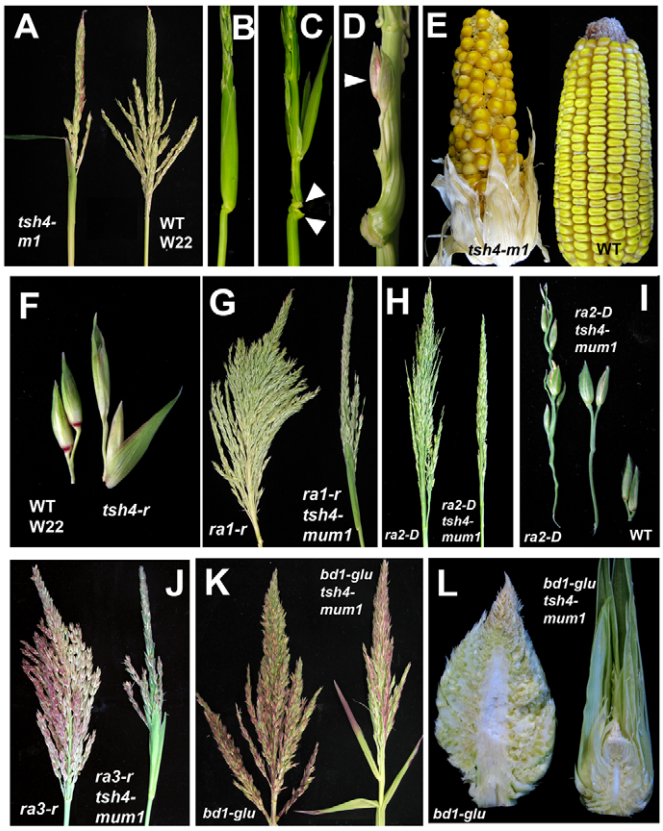

Fig. 1. The maize *tsh4* mutant phenotype and genetic interactions. (**A**) Mature *tsh4-m1* tassels (left) showing fewer branches than in wild-type W22 (right). (**B**) Base of *tsh4-mum1* tassel showing ectopic bract leaves. (**C**) Base of *tsh4-mum1* tassels with bract leaves removed showing compressed nodes (arrowheads). (**D**) Magnification of reduced axillary branch (arrowhead) in the axil of a bract leaf (leaf has been removed). (**E**) Comparison of mature ears of *tsh4-m1* (left) and wild type (right). (**F**) Comparison of mature spikelet pairs of wild-type W22 (left) and *tsh4-r* (right) with ectopic bract. (**G**) Comparison of tassels of *ra1-r* (left) and *ra1-r;tsh4-mum1* (right) showing suppression of the *ra1* phenotype in the double mutant. (**H**) Comparison of tassels of *ra2-DM* (left) and *ra2-DM;tsh4-mum1* (right) showing suppression of the *ra2* phenotype in the double mutant. (**I**) Comparison of spikelet pairs of *ra2-DM* (left) and *ra2-DM;tsh4-mum1* (middle) with wild-type W22 (right). (**J**) Comparison of tassels of *ra3-r* (left) and *ra3-r;tsh4-mum1* (right) showing the suppressed *ra3* phenotype in the double mutant. (**K**) Comparison of tassels of *bd1-glu* (left) and *bd1-glu;tsh4-mum1* (right) showing the additive phenotype in the double mutant. (**L**) Comparison of transverse sections of ears of *bd1-glu* (left) and *bd1-glu;tsh4-mum1* (right) showing the suppressed *bd1* phenotype in the double mutant.

zinc-finger transcription factor (Vollbrecht et al., 2005). *ra3* encodes a trehalose-6-phosphate phosphatase that may also act upstream of *ra1* (Satoh et al., 2006). To determine whether *tsh4* functions within the *ramosa* pathway, double mutants between *tsh4* and *ra1*, *ra2* and *ra3* were made. In all cases, the double mutants appeared *tsh4*-like, displaying fewer tassel branches, indicating that *tsh4* is epistatic to the *ramosa* genes (Fig. 1G-J). *ra2* displayed an additional phenotype of an elongated pedicel, which was not suppressed in the double mutant (Fig. 1I). This might indicate that *tsh4* operates with *ra2* to affect meristem determinacy, rather than stem growth of the pedicel.

The *branched silkless1* (*bd1*) gene, which encodes an ERF-type AP2 transcription factor (Chuck et al., 2002), affects meristem identity. *bd1* mutants display an indeterminate SM in the tassel, whereas in the ear the SM look morphologically like BM (Chuck et al., 2002; Colombo et al., 1998). Double mutants between *bd1* and *tsh4* showed an additive phenotype in the tassel (Fig. 1K), where the number of long branches was reduced as in *tsh4*, but the SMs were indeterminate as in *bd1*. In the ear, however, the *bd1* phenotype was suppressed in double mutants, as the long branches were dramatically shortened and subtended by large bract leaves (Fig. 1L). Thus, the *tsh4* mutant suppresses all BM development, whether in the tassel, as in the *ramosa* mutants, or in the ear, as in *bd1* mutants.

Each double-mutant combination was repeated using the *tsh4-m1* allele, and similar results were observed (data not shown).

Scanning electron microscopy (SEM) analysis

Analysis of *tsh4* development by SEM highlighted differences in meristem initiation and lateral organ suppression in the mutant as compared with the wild type. Normally, in the tassel, the first lateral primordia initiated by the IM are BMs, which have a rounded morphology (Fig. 2A). By contrast, in *tsh4* mutants the first lateral primordia were flattened and later became bract leaves (Fig. 2B). Later, in wild-type tassels, the SPMs are initiated in ordered rows (Fig. 2C), but in *tsh4* the bracts initiated first, and later the SPMs were seen in the axils of the bracts (Fig. 2D). In wild-type ear tips, the bract primordia could be seen prior to the SPMs, but were soon overtaken by growth of the SPMs in the axils, such that no sign of the bract remained by the time SMs were formed (Fig. 2E). In *tsh4* mutants, however, the bract continued to grow, covering the SPM and forcing the rows of SPMs apart, better revealing that the spiral phyllotaxy normally present in wild type was absent due to the lack of internode elongation (Fig. 2F). Together with the double-mutant data, these results demonstrate that *tsh4* is required for BM initiation as well as bract suppression.

Molecular analysis of *tsh4*

Previous work identified a minimum of seven maize SBP-box genes responsible for all aspects of the *Cg1* mutant phenotype (Chuck et al., 2007). Using reverse genetics (Bensen et al., 1995), a *Mutator* transposon insertion was recovered in the last exon of one particular gene, *TC305894* (or *zmSBP6*), that was responsible for the *tsh4-mum1* mutant phenotype. Analysis of two other *tasselsheath* mutants with similar phenotypes identified additional lesions in the same gene. *tsh4-m1* contains a *Dissociation* (*Ds*) transposon insertion within the last exon, whereas the *tsh4-r* allele derived by EMS mutagenesis has a G-to-A transition within the SBP domain that is not present in the progenitor W22 sequence (Fig. 3A). Alignment of the amino acid sequence of the SBP DNA-binding domains of TSH4 and related homologs from maize and other grasses showed a valine-to-methionine transition mutation in the *tsh4-r* product at a highly conserved amino acid (see Fig. S1A in the supplementary material). Analysis of *tsh4* transcripts in the three mutant alleles showed reduced transcript levels in both transposon-induced alleles (Fig. 3B). Together with the fact that all three mutations are allelic (see Materials and methods), these results demonstrate that the *tsh4* mutant phenotype is in fact caused by loss-of-function of *TC305894*. A neighbor-joining tree of related SBP-box genes in maize, rice, *Brachypodium*, sorghum and *Arabidopsis* showed two duplications in the grass family that produced the *tsh4* gene lineage. The first duplication occurred near the base of the grasses, creating two grass clades, whereas a more recent duplication resulted in two maize copies in each of the grass clades (Fig. 3C).

Table 1. Phenotypic analysis of *tsh4* inflorescences

Genotype	Number of branches	Branches with bracts (%)	Solitary spikelets on central spike (%)	Nodes with bracts on central spike (%)	Empty nodes on central spike (%)	Solitary spikelets with bracts on central spike (%)	Paired spikelets with bracts on central spike (%)	Solitary spikelets on branches (%)	Nodes with bracts on branches (%)	Solitary spikelets with bracts on branches (%)	Paired spikelets with bracts on branches (%)
W22	13.8 (0.68)	0 (0)	2.77 (0.63)	0.09 (0.09)	0 (0)	1.67 (1.67)	0 (0)	16.6 (1.66)	0.82 (0.19)	3.17 (0.71)	0.29 (0.18)
tsh4-Ds	5.1 (0.52)	8.17 (3.07)	22.8 (3.26)	18.1 (3.66)	0.12 (0.12)	29.9 (4.27)	15.0 (3.48)	72.8 (2.33)	78.6 (1.28)	72.6 (5.11)	76.2 (3.60)
tsh4-ems	1.5 (0.48)	2.50 (2.26)	53.9 (3.17)	37.4 (10.2)	5.39 (1.8)	38.5 (11.0)	30.6 (9.02)	96.4 (1.50)	93.9 (2.76)	96.6 (1.76)	29.2 (17.2)

Plants were grown to anthesis, then tassels collected and dried. Ten tassels were counted for each genotype (n=10). The mean is shown, with the s.e.m. in parentheses. As the *tsh4* phenotype was consistently stronger in the long tassel branches, as compared with the central spike, these are reported separately.

tsh4 contains an miR156 binding site at the 3′ end of the coding region (Fig. 3A), indicating that it is a target of repression by microRNAs. Although miR156 is temporally regulated and is generally absent during the adult phase of vegetative development (Chuck et al., 2007; Wu and Poethig, 2006), expression reappears within the inflorescence (Fig. 3D). Eleven *MIR156* genes are present in the maize genome (Fig. 3E), but all are more highly expressed in juvenile shoots than inflorescences (Zhang et al., 2009). Recently, a similar microRNA gene, *MIR529*, was described that shares 14-16 bp of homology with *MIR156* and is more highly expressed in tassels than shoots (Zhang et al., 2009). Cleavage analysis of *tsh4* transcripts from wild-type tassels showed that the majority of cleavage (68%) occurred between base pairs 10 and 11 of the predicted microRNA binding site for miR529, whereas 31% occurred near the predicted site for miR156 (Fig. 3F). Thus, miR156 and miR529 function together to repress *tsh4* within inflorescences.

TSH4 expression

To analyze the accumulation TSH4, an antibody was generated against full-length TSH4 protein. This antibody identified a protein present in nuclear extracts of wild-type inflorescences, but not *tsh4-m1* or *Cg1* inflorescences (see Fig. S1B in the supplementary material). *tsh4* RNA was found in a broad domain near the top of the inflorescence in the primordia anlagen, i.e. the position at which primordia initiate. As the primordia grew, the RNA localized to a group of cells adaxial to the SPM, in the position of the suppressed bract (Fig. 4A, arrowhead; see Fig. S1C in the supplementary material). TSH4 antibody localized to the nuclei of cells within the same region (Fig. 4B; see Fig. S1D in the supplementary material), indicating cell autonomy. In addition to being absent from the SPM, no TSH4 was found in the growing BM (Fig. 4C). Within the SM, TSH4 was downregulated, but remained on the abaxial side of the initiating outer glume (Fig. 4D). TSH4 was also present within the inflorescence stem (Fig. 4C,D), but not in the IM itself, nor in any other lateral meristems. Using the same antibody on the *tsh4-m1* allele, no staining was detectable (Fig. 4E), indicating that the antibody was specific to TSH4. Overall, the location of TSH4 appeared to mark both stem and repressed bract, but not meristem.

It is curious that TSH4 marked the position of lateral primordia and was required for the normal number of branches and spikelet pairs, but was never found in meristems. To determine whether *tsh4* does in fact play a role in marking and establishing meristem boundaries, double labeling of TSH4 and several meristem markers was performed. Expression of the *knotted1* (*kn1*) homeobox gene marked all shoot meristems (Jackson et al., 1994), and double labeling of *kn1* RNA and TSH4 showed that *kn1* and TSH4 did not overlap in the IM and BM (Fig. 4F,G). Radial sections through the tassel tip at the point of SPM initiation showed that *kn1* was expressed in an internal domain in the stem, whereas TSH4 was found adjacent to it, external to the *kn1* domain. Interestingly, *kn1* was absent from the anlagen of the SPM, but present later as the SPM developed (Fig. 4G). This is consistent with a role for *kn1* in maintaining the growth of meristems, rather than in their initiation (Hake et al., 2004).

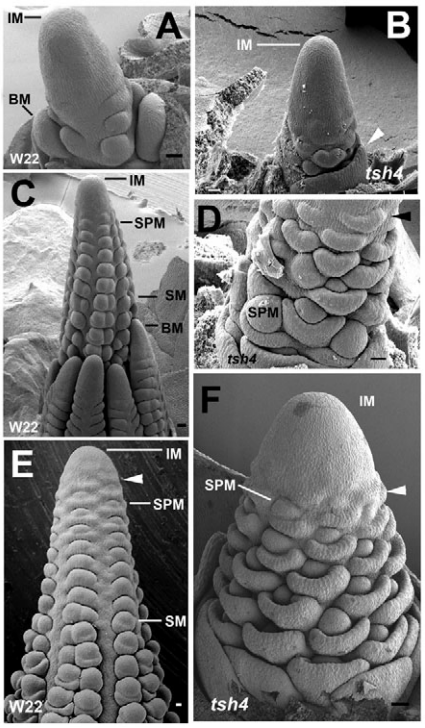

Fig. 2. Scanning electron micrographs of *tsh4-m1* and wild-type W22. (**A**) Early-stage wild-type tassel showing branch meristem initiation. (**B**) Early-stage *tsh4* tassel lacking BM and showing bract initiation (arrowhead). (**C**) Later-stage wild-type W22 tassel showing ordered rows of lateral primordia. (**D**) Later-stage *tsh4* tassel showing precocious initiation of bract primordia (arrowhead) and axillary meristems. (**E**) Later-stage wild-type ear primordium displaying rows of primordia. Suppressed bracts are evident near the tip (arrowhead). (**F**) Later-stage *tsh4* ear primordium showing precocious bract development (arrowhead) and spiral phyllotaxy of lateral primordia. BM, branch meristem; IM, inflorescence meristem; SM, spikelet meristem; SPM, spikelet pair meristem. Scale bars: 40 μm.

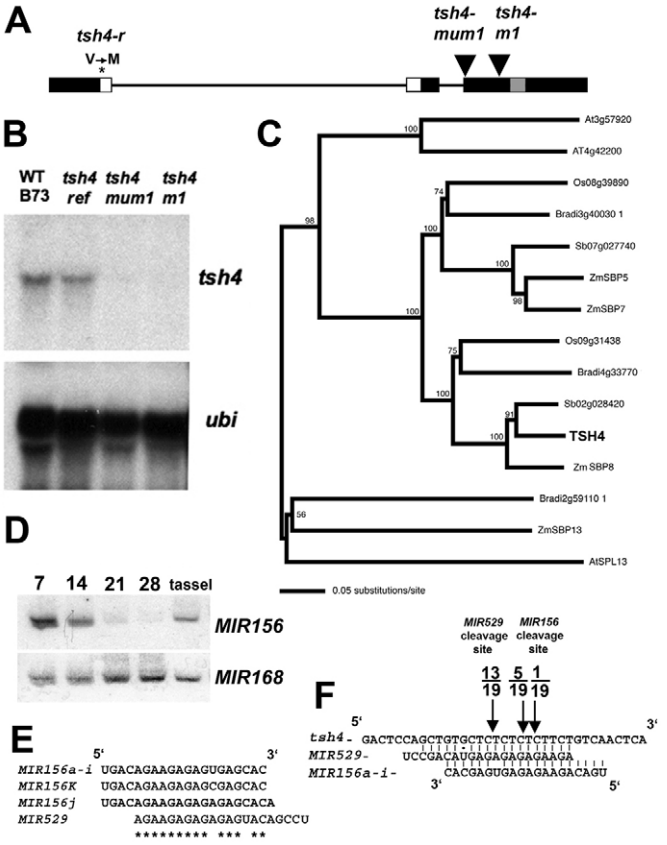

Fig. 3. Structure and molecular analysis of *tsh4*. (**A**) Genomic structure of maize *tsh4*. Black boxes are exons, lines are introns, white boxes represent the SBP-box domain, and the gray box is the miR156 binding site. Black triangles represent transposon insertions. (**B**) Northern blot analysis of *tsh4* expression. Total RNA was extracted from 0.5 cm ear primordia from the wild type and three *tsh4* alleles and probed with the 3′ end of the *tsh4* cDNA. (**C**) Neighbor-joining tree of *tsh4*-like SBP-box genes from rice (Os), *Brachypodium* (Brad), sorghum (Sb), maize (Zm) and *Arabidopsis* (At). (**D**) MicroRNA northern blot with shoot RNA from 7 to 28 days after planting and 0.5 cm tassel primordia. miR156 disappears at the adult phase transition, but returns in inflorescence tissue. (**E**) Alignment of miR156 family sequences with miR529. miR529 shares 14-16 nt in common with miR156. (**F**) Cleavage of *tsh4* transcript in tassels by miR529 and miR156. The number of clones cleaved at each position over total clones analyzed is indicated above the arrows. Greater than 68% of the clones were cleaved at the predicted miR529 cleavage site.

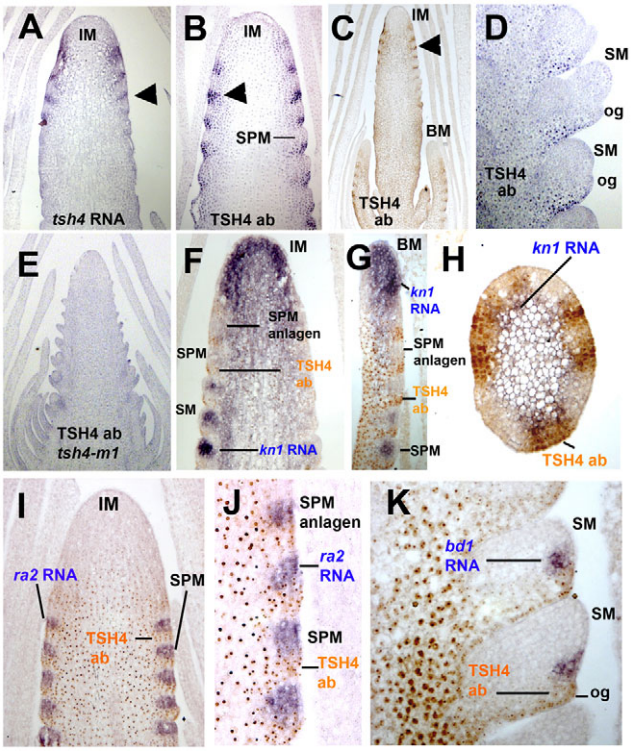

Fig. 4. Analysis of wild-type *tsh4* expression by in situ hybridization and immunolocalization. (**A**) Tassel primordium probed with *tsh4* RNA. Expression is located at the base of the SPM (arrowhead). (**B**) Tassel primordium probed with TSH4 antibody (ab) and developed with chromogenic substrate NBT/BCPIP (blue). Expression is located at the base of the SPM (arrowhead) in a similar location to the RNA. (**C**) Tassel primordium with branches probed with the TSH4 antibody and developed with DAB (gold). No protein is evident in any lateral or terminal meristems. (**D**) Older tassel primordium with initiating spikelets probed with TSH4 antibody. Upon initiation of the outer glume (og), downregulation of TSH4 is evident within the SM. (**E**) *tsh4-m1* mutant probed with TSH4 antibody. Little or no TSH4 protein is present. (**F**) Double labeling of tassel primordium with *kn1* RNA (blue) and TSH4 antibody (gold) showing complementary expression. (**G**) Magnification of tassel branch with double labeling with *kn1* RNA (blue) and TSH4 antibody (gold) showing lack of *kn1* in early SPM. (**H**) Radial section of IM showing adjacent expression of *kn1* RNA (blue) in inner stem, and TSH4 protein (gold) in the outer stem. (**I**) Double labeling of tassel primordium with *ra2* RNA (blue) and TSH4 antibody (gold) showing complementary expression in the SPM. (**J**) Magnification of double labeling of tassel primordium with *ra2* RNA (blue) and TSH4 antibody (gold) showing overlapping expression in the SPM anlagen and complementary expression in the SPM. (**K**) Double labeling of the SM with *bd1* RNA (blue) and TSH4 antibody (gold) showing lack of TSH4 at the boundary established by *bd1*.

To assay the overlap between the initiating SPM and TSH4 accumulation, double labeling with the lateral meristem marker *ra2* was performed (Fig. 4I). *ra2* was expressed in the SPM anlagen, transiently in the SPM and SM, but not in the FM or bracts (Bortiri et al., 2006). Unlike the result with *kn1*, a clear overlap between *ra2* expression and TSH4 occurred in the SPM anlagen, but later resolved into complementary domains (Fig. 4J), pointing to an early role for TSH4 in controlling primordium fate. Finally, to understand the role of TSH4 in the establishment of the SM, double labeling with the SM-specific marker *bd1* (Chuck et al., 2002) and TSH4 was assayed. In normal plants, *bd1* transcripts first appear in the axil of the initiating outer glume at the base of the SM. TSH4 protein did not overlap with *bd1* in this domain (Fig. 4K), and may be excluded from this area in wild type (Fig. 4D). Together, these results show that TSH4 is expressed in a pattern that is complementary to lateral meristems such as the BM and SM, but which transiently overlaps in the early SPM.

Factors that negatively regulate *tsh4*

Meristem-specific factors are likely to downregulate *tsh4*, as downregulation of TSH4 was not observed in mutants that fail to initiate lateral meristems, such as *barren1* (*ba1*) (Fig. 5A) (Ritter et

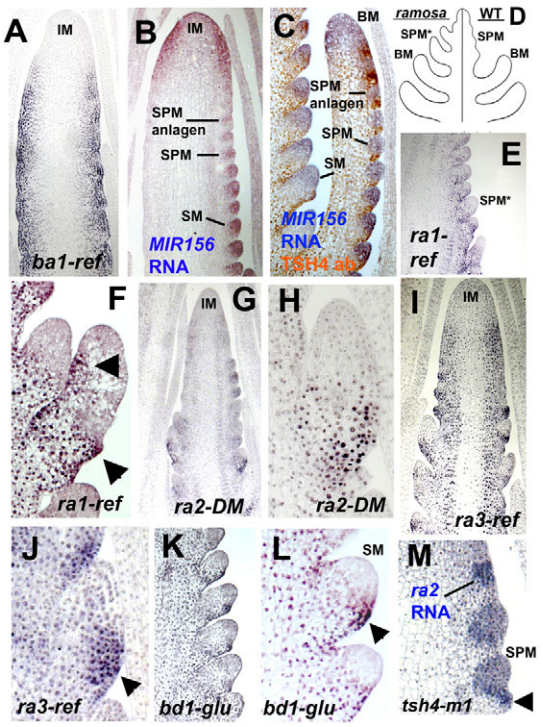

Fig. 5. Analysis of *MIR156* and *tsh4* expression in branching mutants. (**A**) Analysis of TSH4 in a *ba1* mutant tassel. No downregulation of TSH4 is seen in lateral positions. (**B**) Detection of miR156 in wild-type tassels, showing hybridization in all meristems. To simplify labeling, miR529 is grouped into the miR156 family as both are highly similar and share the same targets. (**C**) Double labeling of miR156 (blue) and TSH4 (gold) in wild-type tassel with branch. Their expression patterns appear complementary. (**D**) Schematic of wild-type (right) compared with *ramosa* (left) tassel development. The mutant SPM (SPM*) is indeterminate and branch-like in *ra1*, *ra2* and *ra3* mutants. In *bd1* mutants (not shown), the mutant SM is similarly indeterminate and branch-like. (**E**) *ra1-ref* tassel primordium probed with TSH4 antibody. (**F**) Magnification of *ra1-ref* indeterminate SPM showing ectopic TSH4 localization on the abaxial and adaxial sides of the branch (arrowheads). (**G**) *ra2-DM* tassel primordium probed with TSH4 antibody. (**H**) Magnification of *ra2-DM* indeterminate SPM showing ectopic TSH4 localization on the abaxial side of the branch. (**I**) *ra3-ref* tassel primordium probed with TSH4 antibody. (**J**) Magnification of *ra3-ref* indeterminate SPM showing ectopic TSH4 localization on the abaxial side of the branch (arrowhead). (**K**) *bd1-glu* ear primordium probed with TSH4 antibody. (**L**) Magnification of *bd1-glu* ear spikelets showing ectopic abaxial TSH4 localization at the base of the SM (arrowhead). (**M**) In situ hybridization of *tsh4-m1* ear with *ra2* RNA showing ectopic expression in derepressed bract (arrowhead).

al., 2002). We carried out in situ hybridizations using a locked nucleic acid (LNA) probe that is complementary to miR156 and likely also to hybridize to miR529 (Fig. 5B). Expression of miR156/miR529 was seen in all meristems of the inflorescence in a pattern complementary to that of TSH4 (Fig. 5C). The expression domains were complementary, not overlapping, suggesting that miR156/miR529 does in fact regulate TSH4.

Our genetic and double-labeling results suggest that the *ramosa* genes and *bd1* might also negatively regulate *tsh4*. All *ramosa* mutants display indeterminate SPMs that appear branch-like compared with wild type (Fig. 5D). Immunolocalization showed that the TSH4 domain is much larger in a *ra1* background than in wild type. TSH4 protein was detected on the abaxial side of the indeterminate SPM in the *ra1-ref* allele (Fig. 5E). As the *ra1* mutant SPM grew, ectopic TSH4 protein was also detected on the adaxial side of the indeterminate SPM (Fig. 5F), co-incident with *ra1* expression (Vollbrecht et al., 2005). In a *ra2* mutant background, ectopic TSH4 protein was also observed in indeterminate SPMs (Fig. 5G), although the localization was mostly abaxial (Fig. 5H). Abaxial ectopic TSH4 in indeterminate SPMs was also seen in *ra3* backgrounds (Fig. 5I,J). Finally, ectopic TSH4 was observed in *bd1* mutant SMs that morphologically resemble BMs (Fig. 5K). Abaxial ectopic localization of TSH4 was observed in the region of the *bd1* SM that would normally form glumes and lack TSH4 in wild type (Fig. 5L). Taken together, these results might indicate that *ramosa* and *bd1* genes directly or indirectly negatively regulate TSH4 protein accumulation to regulate branch growth.

To determine whether the converse is true, i.e. whether TSH4 negatively regulates the *ramosa* genes, we carried out in situ hybridizations on *tsh4* mutants. As shown in Fig. 5M, *ra2* transcript was ectopically expressed in *tsh4-m1* bracts, indicating mutual negative regulation between *ra2* and *tsh4*. By contrast, no ectopic expression of *ra1* or *ra3* was observed in *tsh4* backgrounds (G.C., unpublished).

DISCUSSION

Plant architecture can be viewed as a repeating series of phytomers, each of which contains three components: a leaf, axillary meristem and internode. Cell lineage analyses have shown that the phytomer can be considered a compartment, as clonal sectors transverse the entire phytomer and end at phytomer boundaries (Johri and Coe, 1983). It follows that the cells within the phytomer may share a common origin, and that subsequent cell fate decisions fix the cells into their separate identities. By altering the balance of cells within the phytomer unit and controlling how they are partitioned to each component, it is possible to create the wide range of morphological variation found in grass inflorescences.

We show that the *tsh4* gene plays a major role in establishing domains within the phytomer. Floral bracts are derepressed at the base of both long branches and spikelet pairs, resulting in fewer of each in the mutant (Fig. 1; Table 1). This derepressed bract growth occurs at the expense of the axillary meristem, as more cells are allocated for lateral organ growth than meristem growth, thus reducing meristem potential. The ectopic expression of lateral meristem markers, such as *ra2*, in the bracts of the *tsh4-m1* mutant (Fig. 5M) supports the idea that meristems with reduced growth potential result from misallocation of SPM cells into the growing bract. Since TSH4 is found adjacent to meristem boundaries (Fig. 4F-K), misallocation of cells might result from the lack of establishment of a boundary between meristem and lateral organ. The derepressed bract growth also alters the apparent phyllotaxy, changing it from ordered rows to spiral by pushing the rows of spikelet pairs apart (Fig. 3F). This suite of phenotypes is found in the dominant *Cg1* mutant and suggests that loss of expression of *tsh4*-related genes is likely to be the primary cause of the diverse floral defects observed in *Cg1* inflorescences (Chuck et al., 2007).

Genes related to *tsh4* in *Arabidopsis* regulate the duration of leaf initiation (plastochron) (Schwarz et al., 2008; Wang et al., 2008). *SPL9* and *SPL15* are functionally redundant and display an increased rate of vegetative leaf initiation in the double mutant. In addition, the double mutants have more branches (Schwarz et al., 2008), a phenotype also seen in miR156 overexpressers in *Arabidopsis* (Schwab et al., 2005). The opposite phenotype, a decrease in the rate of leaf initiation, is obtained when a microRNA-

resistant version of *SPL9* is expressed from various promoters (Wang et al., 2008). Similar to *tsh4*, the *SPL9* transcript is found in the stem and young leaf primordia and is absent from meristems (Wang et al., 2008). Using different domain-specific promoters to drive *SPL9* expression, it was found that the effects on plastochron occurred when driven by lateral organ-specific promoters. These results suggested to the authors that the *SPL9* effects on plastochron occur non-cell-autonomously (Wang et al., 2008). Our results, however, indicate that it is unlikely that TSH4 itself functions non-cell-autonomously, as the protein and RNA coincide in the anlagen of lateral organ primordia.

Although both the maize *tsh4* mutant and the *Arabidopsis spl9;spl15* double mutant have more leaves than wild type, there are striking differences in function. Axillary branch number increased with the increase in leaf number in the *spl9;spl15* plants (Schwarz et al., 2008), but *tsh4* mutants, by contrast, exhibit a loss of axillary branch growth concomitant with growth of the depressed bract. Despite initiating many extra leaves, *spl9;15* mutants do not display an overall difference in meristem size (Schwarz et al., 2008), whereas *tsh4* mutants initiate fewer lateral meristems with reduced growth potential. In *Arabidopsis*, there is no derepression of cryptic bract growth or compensatory growth in the components of the phytomer in the double mutant, whereas in maize derepressed bract leaves grow at the expense of the axillary meristem. It appears that the miR156/*SPL* cassette was recruited in maize to function specifically to balance the decision to be leaf versus meristem in axillary locations, whereas the same cassette functions in the shoot apex of *Arabidopsis* to regulate the timing of leaf initiation.

In rice, the *NECK LEAF1* (*NL1*) gene affects both plastochron and phytomer. *nl1* mutants display a shortened plastochron, are slightly dwarfed, have overgrown bracts at the base of primary branches, smaller panicles and fewer branches (Wang et al., 2009). *NL1* encodes a GATA transcription factor similar to that encoded by *HANABA TARANU* (*HAN*) (Zhao et al., 2004). *NL1* is expressed within inflorescence bract primordia and is likely to regulate *PLA1*, which encodes a cytochrome P450 monooxygenase that controls plastochron (Miyoshi et al., 2004). The fact that *HAN* mutants in *Arabidopsis* display no bract phenotypes indicates that monocotyledonous plants have evolved a unique set of genes to control bract suppression during the floral phase. *tasselsheath1* is the maize ortholog of *NL1* (C.W., unpublished), but is likely to operate genetically in a parallel pathway to *tsh4* (data not shown).

Although *tsh4* is not expressed in meristems, the double-mutant data clearly indicate that *tsh4* plays a role in lateral meristem initiation. Plants that are mutant for both *tsh4* and *ra1*, *ra2*, *ra3* and *bd1*, which alone are highly branched maize mutants, exhibit a *tsh4* phenotype (Fig. 1G-L), demonstrating that BM growth requires *tsh4* gene function. The ectopic expression of *tsh4* in the abaxial domain of the BM-like SPM of *ra1*, *ra2*, *ra3* (Fig. 5E-J), or in the BM-like SM of *bd1* (Fig. 5K,L), provides insight into the mechanism by which *tsh4* may indirectly affect BM activity. Indeterminate growth of BMs in highly branched mutants or wild-type tassel branches might require *tsh4* gene activity to suppress bract development. Otherwise, misallocation of cells into derepressed bracts would decrease meristem potential of the branch, thus inhibiting its growth. When *tsh4* is active, the cells of the repressed bract are incorporated into the growing stem, allowing extended branch elongation. This is shown by the discrete TSH4 accumulation on the faster growing, abaxial side of the indeterminate branches of all *ramosa* mutants as well as of *bd1* (Fig. 5F,H,J,L). *tsh4*, however, is not required for growth of the stem itself, as *tsh4* mutants still have stems and do not suppress the elongated pedicel stem phenotype of the *ra2-DM* mutant (Fig. 1I). Thus, the primary function of *tsh4* is to repress outgrowth of bract primordia within the inflorescence, causing the cells that express it to be incorporated into the stem, therefore allowing extended branch growth.

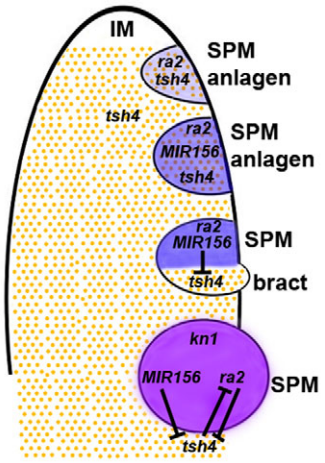

Fig. 6. Model for early maize inflorescence patterning by negative regulation of TSH4. Early expression of *ra2* and TSH4 overlap in the SPM anlagen, but repression of TSH4 by miR156 at later stages restricts TSH4 to the bract, where it suppresses growth. Upon establishment of the growing SPM, *kn1* is expressed while *ra2* and *tsh4* mutually repress one another in adjacent domains. Gold dots, TSH4 protein; light blue, *ra2* expression; darker blue, miR156 expression plus *ra2* expression; purple, *kn1*, *ra2* and *kn1* expression.

Different factors are required for the regulation of *tsh4* during early and late SPM development. A major early factor negatively regulating *tsh4* function is miR156 and the closely related miR529. *Arabidopsis* SPL transcription factors are known to be regulated by miR156 at the level of translation (Gandikota et al., 2007), thus necessitating the need for antibodies to analyze *SPL* gene expression. TSH4 protein was excluded from all meristems, whereas expression of miR156 was complementary, being specific to meristems, strongly suggesting that miR156 and miR529 function to restrict TSH4 from meristems. Thus, miR156 and miR529 play a major role in the establishment of inflorescence architecture by downregulating *tsh4* within the SPM anlagen where *tsh4* and *ra2* expression coincide (Fig. 6), and by limiting *tsh4* activity to the stem and bract, where it suppresses development. Once the SPM boundary has been established and the meristem begins to grow, *kn1* expression initiates to maintain the meristem (Fig. 6). Mutual negative regulation between *ra2* and *tsh4* occurs in adjacent domains, as demonstrated by the ectopic expression of *ra2* in the derepressed bracts of *tsh4* mutants (Fig. 5M). *ra2*, however, also represses *tsh4*, as *tsh4* is epistatic to *ra2* (Fig. 1H) and TSH4 is ectopically expressed in *ra2* mutants (Fig. 5H). Mutual negative regulatory loops are a common feature of transcription factor biology (Crews and Pearson, 2009) and might serve as a mechanism to reinforce developmental boundaries.

The effects of *tsh4* on plant development demonstrate that the phytomer behaves as a single unit that is difficult to subdivide into individual components. Although *tsh4* is expressed in only a subset of the phytomer, it affects growth, initiation and phyllotaxy of every aspect of the phytomer by repressing cell growth and

differentiation in a specific domain, thus allowing compensatory growth in other parts. Since at least three closely related *tsh4*-like genes are present in the maize genome (Fig. 3C; see Fig. S1A in the supplementary material), it is likely that they also have phytomer functions. One of these genes, *zmSBP8*, is likely to be a duplicate of *tsh4*, although it is expressed at lower levels (data not shown), which might explain why *tsh4* alone displays a phenotype. Nevertheless, the isolation of mutations in these genes will provide a clearer picture of how growth of the various phytomer components is coordinated.

Acknowledgements
We thank China Lunde and Nathalie Buldoc for reviewing the manuscript; Bob Meeley for the gift of the *tsh4-mum1* allele; De Woods for use of the scanning electron microscope; and David Hantz for greenhouse support. This work was supported by DOE grant DE-A102-08ER15962 and BARD grant IS-4249-09.

Competing interests statement
The authors declare no competing financial interests.

Supplementary material
Supplementary material for this article is available at
http://dev.biologists.org/lookup/suppl/doi:10.1242/dev.048348/-/DC1

References

Bensen, R. J., Johal, G. S., Crane, V. C., Tossberg, J. T., Schnable, P. S., Meeley, R. B. and Briggs, S. P. (1995). Cloning and characterization of the maize *An1* gene. *Plant Cell* **7**, 75-84.
Bortiri, E., Chuck, G., Vollbrecht, E., Rocheford, T. F., Martienssen, R. and Hake, S. (2006). *ramosa2* encodes a Lateral Organ Boundary domain protein that determines the fate of stem cells in branch meristems of maize. *Plant Cell* **18**, 574-585.
Cheng, P. C., Greyson, R. I. and Walden, D. B. (1983). Organ initiation and the development of unisexual flowers in the tassel and ear of *Zea mays*. *Am. J. Bot.* **70**, 450-462.
Chuck, G., Meeley, R. and Hake, S. (1998). The control of maize spikelet meristem fate by the *APETALA2*-like gene *indeterminate spikelet1*. *Genes Dev.* **12**, 1145-1154.
Chuck, G., Muszynski, M., Kellogg, E., Hake, S. and Schmidt, R. J. (2002). The control of spikelet meristem identity by the branched silkless1 gene in maize. *Science* **298**, 1238-1241.
Chuck, G., Cigan, M., Saeteurn, K. and Hake, S. (2007). The heterochronic maize mutant Corngrass1 results from overexpression of a tandem microRNA. *Nat. Genet.* **39**, 544-549.
Colombo, L., Marziani, G., Masiero, S., Wittich, P. E., Schmidt, R. J., Gorla, M. S. and Pe, E. M. (1998). *Branched silkless* mediates the transition from spikelet to floral meristem during *Zea mays* ear development. *Plant J.* **16**, 353-363.
Crews, S. T. and Pearson, J. C. (2009). Transcriptional autoregulation in development. *Curr. Biol.* **19**, 241-246.
Dinneny, J. R., Yadegari, R., Fischer, R. L., Yanofsky, M. F. and Weigel, D. (2004). The role of JAGGED in shaping lateral organs. *Development* **131**, 1101-1110.
Galinat, W. C. (1959). The phytomer in relation to the floral homologies in the American Maydea. *Bot. Mus. Lefl., Harv. Univ.* **19**, 1-32.
Gandikota, M., Birkenbihl, R. P., Hohmann, S., Cardon, G. H., Saedler, H. and Huijser, P. (2007). the miRNA156/157 recognition element in the 3'UTR of the Arabidopsis SBP box gene SPL3 prevents early flowering by translational inhibition in seedlings. *Plant J.* **49**, 683-693.
Hake, S., Smith, H. M. S., Holtan, H., Magnani, E., Mele, G. and Ramirez, J. (2004). The role of *KNOX* genes in plant development. *Annu. Rev. Cell Dev. Biol.* **20**, 125-151.
Heisler, M. G., Ohno, C., Das, P., Sieber, P., Reddy, G. V., Long, J. A. and Meyerowitz, E. M. (2005). Patterns of auxin transport and gene expression during primordium development revealed by live imaging of the Arabidopsis inflorescence meristem. *Curr. Biol.* **15**, 1899-1911.
Hempel, F. D. and Feldman, L. J. (1994). Bi-directional inflorescence development in *Arabidopsis thaliana*: acropetal initiation of flowers and basipetal initiation of paraclades. *Planta* **192**, 276-286.
Hempel, F. D. and Feldman, L. J. (1995). Specification of chimeric flowering shoots in wild-type *Arabidopsis*. *Plant J.* **8**, 725-731.
Hepworth, S. R., Zhang, Y., McKim, S., Li, X. and Haughn, G. W. (2005). BLADE-ON-PETIOLE-dependent signaling controls leaf and floral patterning in Arabidopsis. *Plant Cell* **17**, 1434-1448.
Hepworth, S. R., Klenz, J. E. and Haughn, G. W. (2006). UFO in the Arabidopsis inflorescence apex is required for floral-meristem identity and bract suppression. *Planta* **223**, 769-778.
Jackson, D. (1991). In situ hybridization in plants. In *Molecular Plant Pathology: A Practical Approach* (ed. D. J. Bowles, S. J. Gurr and M. McPherson), pp. 163-174. Oxford: Oxford University Press.
Jackson, D., Veit, B. and Hake, S. (1994). Expression of maize *KNOTTED1* related homeobox genes in the shoot apical meristem predicts patterns of morphogenesis in the vegetative shoot. *Development* **120**, 405-413.
Johri, M. M. and Coe, E. H. (1983). Clonal analysis of corn plant development. I. The development of the tassel and the ear shoot. *Dev. Biol.* **97**, 154-172.
Kerstetter, R., Vollbrecht, E., Lowe, B., Veit, B., Yamaguchi, J. and Hake, S. (1994). Sequence analysis and expression patterns divide the maize *knotted1*-like homeobox genes into two classes. *Plant Cell* **6**, 1877-1887.
McSteen, P. (2006). Branching out: the ramosa pathway and the evolution of grass inflorescence morphology. *Plant Cell* **18**, 518-522.
Miyoshi, K., Ahn, B., Kawakatsu, T., Ito, Y., Itoh, J., Nagato, Y. and Kurata, N. (2004). PLASTOCHRON1, a timekeeper of leaf initiation in rice, encodes cytochrome. P450. *Proc. Natl. Acad. Sci. USA* **101**, 875-880.
Norberg, M., Holmlund, M. and Nilsson, O. (2005). The BLADE ON PETIOLE genes act redundantly to control the growth and development of lateral organs. *Development* **132**, 2203-2213.
Ohno, C. K., Reddy, G. V., Heisler, M. G. and Meyerowitz, E. M. (2004). The Arabidopsis JAGGED gene encodes a zinc finger protein that promotes leaf tissue development. *Development* **131**, 1111-1122.
Poethig, R. S. (1988). Heterochronic mutations affecting shoot development in maize. *Genetics* **119**, 959-973.
Ritter, M. K., Padilla, C. M. and Schmidt, R. J. (2002). The maize mutant, barren stalk 1, is defective in axillary meristem development. *Am. J. Bot.* **89**, 203-210.
Satoh, N., Nagasawa, N., Malcomber, S., Sakai, H. and Jackson, D. (2006). A trehalose metabolic enzyme controls inflorescence architecture in maize. *Nature* **441**, 227-230.
Schwab, R., Palatnik, J. F., Riester, M., Schommer, C., Schmid, M. and Weigel, D. (2005). Specific effects of microRNAs on the plant transcriptome. *Dev. Cell* **8**, 517-527.
Schwarz, S., Grande, A. V., Bujdoso, N., Saedler, H. and Huijser, P. (2008). The microRNA regulated SBP-box genes SPL9 and SPL15 control shoot maturation in Arabidopsis. *Plant Mol. Biol.* **67**, 183-195.
Vollbrecht, E., Springer, P. S., Goh, L., Buckler, E. S. and Martienssen, R. (2005). Architecture of floral branch systems in maize and related grasses. *Nature* **436**, 1119-1126.
Wang, J. W., Schwab, R., Czech, B., Mica, E. and Weigel, D. (2008). Dual effects of miR156-targeted SPL genes and CYP78A5/KLUH on plastochron length and organ size in Arabidopsis thaliana. *Plant Cell* **20**, 1231-1243.
Wang, L., Yin, H., Qian, Q., Yang, J., Huang, C., Hu, X. and Luo, D. (2009). NECK LEAF 1, a GATA type transcription factor, modulates organogenesis by regulating the expression of multiple regulatory genes during reproductive development in rice. *Cell Res.* **19**, 598-611.
Weigel, D., Alvarez, J., Smyth, D. R., Yanofsky, M. F. and Meyerowitz, E. M. (1992). LEAFY controls floral meristem identity in Arabidopsis. *Cell* **69**, 843-859.
Wu, G. and Poethig, R. S. (2006). Temporal regulation of shoot development in Arabidopsis thaliana by miR156 and its target SPL3. *Development* **133**, 3539-3547.
Zhang, L., Chia, J., Kumari, S., Stein, J., Liu, Z., Narechania, A., Maher, C., Guill, K., McMullen, M. and Ware, D. (2009). A genome-wide characterization of microRNA genes in maize. *PLoS Genet.* **5**, e1000716.
Zhao, Y., Medrano, L., Ohashi, K., Fletcher, J., Yu, H., Sakai, H. and Meyerowitz, E. (2004). HANABA TARANU is a GATA transcription factor that regulates shoot apical meristem and flower development in Arabidopsis. *Plant Cell* **16**, 2586-2600.